Unveiling Non-Uniform Parameter Tuning Rules in Heterogeneous Multi-converter Power Systems: Value Set Based Robust Stability Assessment

1st Zhongyu Fu
Polytechnic Institute
Zhejiang University
Hangzhou, China
email: 22460689@zju.edu.cn

2nd Zhichao Zhou
Zhejiang Electric Power Design Institute Co., Ltd.
China Energy Engineering Group
Hangzhou, China
email: xyz_power@163.com

3rd Jiaoting Kuang
Zhejiang Electric Power Design Institute Co., Ltd.
China Energy Engineering Group
Hangzhou, China
email: juven1997@163.com

4th Yu Tang
Polytechnic Institute
Zhejiang University
Hangzhou, China
email: eeyutang@zju.edu.cn

5th Huisheng Gao
College of Electrical Engineering
Zhejiang University
Hangzhou, China
email: gaohuisheng@zju.edu.cn

6th Huanhai Xin
College of Electrical Engineering
Zhejiang University
Hangzhou, China
email: xinhh@zju.edu.cn

***Abstract*—To address the challenges of complex interactive coupling and robust stability analysis caused by parameter heterogeneity in Phase-Locked Loop-dominated Heterogeneous Multi-converter Power Systems (HMCS), this paper proposes a robust stability assessment and control parameter optimization strategy for HMCS based on value set theory. First, an accurate and low-dimensional uncertainty separation model for HMCS is established. Secondly, by combining this model with value set theory, a robust stability analysis method and a clear parameter tuning strategy for HMCS are proposed. Then, the proposed method is applied to analyze the impact of HMCS parameters on system strength. Finally, simulation results validate the effectiveness of the proposed method. The analysis results indicate that the parameter tuning rules in HMCS no longer follow the experience from single-converter systems. Identical types of control parameters from different converters may have opposite effects on system strength, highlighting that precise parameter tuning decisions are crucial for enhancing system strength.**

***Index Terms*—control parameter optimization, heterogeneous multi-converter power systems, robust stability, small-signal stability**

I. Introduction

With the increasing penetration of renewables in weak grids, the dynamic interaction between Phase-Locked Loop (PLL)-dominated Grid-Following (GFL) converter control systems and the power grid has become a primary cause of low- and medium-frequency oscillation and small-signal instability problems [1]. Actual power systems often contain converters from different manufacturers with varying control parameters, forming Heterogeneous Multi-converter Power Systems (HMCS). This heterogeneity complicates the system's dynamic characteristics, making the impact of interactions between different converters on system stability difficult to assess directly and lacking a basis for parameter tuning. The small-signal stability margin dominated by PLL dynamics is referred to as system strength, which is closely related to the Proportional-Integral (PI) parameters of the PLL. The parameter tuning considered hereafter in this paper mainly refers to the PLL's PI parameters.

The small-signal stability assessment of PLL-dominated HMCS has been extensively investigated, utilizing methods such as state-space and modal analysis, admittance matrix methods, and generalized short-circuit ratio indices [2]–[4]. However, existing methods primarily evaluate the system's nominal small-signal stability, with less focus on the robust stability issues arising from parameter heterogeneity. Furthermore, in terms of parameter tuning, although studies on single-converter systems have shown that increasing the PLL's proportional gain and decreasing the integral gain enhances system strength [5], the applicability of this conclusion in HMCS remains questionable. Due to the diverse parameters of converters and the complex inter-converter coupling in HMCS, simply applying the unified tuning strategies from homogeneous systems may be ineffective.

The value set approach, based on polynomial theory, has shown potential in robust stability analysis [6]. By plotting the value set, which maps the uncertain parameter space onto a two-dimensional complex plane, the robust stability of the system can be intuitively judged. However, the value set method requires the uncertainty structure to be completely separated and lacks specific modeling and parameter variation guidance tailored to PLL-dominated small-signal stability problems.

This work is supported by China Energy Engineering Group Zhejiang Electric Power Design Institute Co., Ltd. under Project "Research on Inertia Response and Oscillation Damping Provided by Energy Storage for Power Grids" (No. WD2025KJ230601).

979-8-3315-8138-1

To address the limitations of existing methods, this paper proposes a robust stability assessment and enhancement strategy for PLL-dominated HMCS. The main contributions are: (1) A low-dimensional and approximation-free uncertainty separation model for HMCS is established. (2) Combining the established model with the value set method, a robust stability analysis procedure for HMCS is proposed, and a clear basis for parameter tuning is established accordingly. (3) The application of this method reveals the unique complexity of HMCS parameter tuning: unlike single-converter systems, no unified parameter tuning strategy exists for HMCS.

The remainder of this paper is organized as follows: Section II details the uncertainty modeling. Section III presents the robust stability analysis method and parameter tuning guidelines. Section IV validates the proposed strategy through case studies, revealing the non-uniform tuning rules of heterogeneous systems. Section V concludes the paper.

II. HMCS Uncertainty Separation Modeling

A. Uncertainty Representation of HMCS Characteristic Matrix

Consider an HMCS system containing n GFL converters. Its dynamic behavior can be described by the converter models and the grid model. Consider the robust analysis ranges for the PI parameters k_{pj} and k_{ij} in the j-th converter model as $[k_{ij}^{\min}, k_{ij}^{\max}]$ and $[k_{pj}^{\min}, k_{pj}^{\max}]$, respectively. For ease of analysis, the PI parameters of the converter are normalized:

$$\begin{aligned} k_{pj} &= k_{pj0} + \Delta k_{pj}\delta_{pj} \\ k_{ij} &= k_{ij0} + \Delta k_{ij}\delta_{ij} \end{aligned} \tag{1}$$

where $\delta_{pj}, \delta_{ij} \in [-1, 1]$ represent the normalized uncertain variables of the PI parameters, k_{pj0} and k_{ij0} represent the nominal parameter values, and Δk_{pj} and Δk_{ij} represent the parameter adjustment ranges.

This paper adopts the widely validated second-order reduced-order PLL model to describe the dynamic characteristics of the j-th converter. This model is suitable for analyzing PLL-dominated low- and medium-frequency oscillation problems [7]. Considering parameter uncertainty, its linearized state-space expression is:

$$\begin{aligned} \Delta\dot{\boldsymbol{X}}_j &= \boldsymbol{A}_j(\boldsymbol{\delta})\Delta\boldsymbol{X}_j + \boldsymbol{B}_j(\boldsymbol{\delta})\Delta\boldsymbol{U}_j \\ \Delta\boldsymbol{I}_j &= S_{Bj}\boldsymbol{C}_j\Delta\boldsymbol{X}_j \end{aligned} \tag{2}$$

where:

$$\begin{aligned} &\boldsymbol{A}_j(\boldsymbol{\delta}) = \boldsymbol{A}_{j0} + \boldsymbol{\delta}_j\boldsymbol{A}_{j1}, \quad \boldsymbol{B}_j(\boldsymbol{\delta}) = \boldsymbol{B}_{j0} + \boldsymbol{\delta}_j\boldsymbol{B}_{j1} \\ &\boldsymbol{A}_{j0} = \begin{bmatrix} 0 & -k_{ij0}U_{j0} \\ 1 & -k_{pj0}U_{j0} \end{bmatrix}, \quad \boldsymbol{B}_{j0} = \frac{1}{U_{j0}}\begin{bmatrix} -k_{ij0}U_{yj0} & k_{ij0}U_{xj0} \\ -k_{pj0}U_{yj0} & k_{pj0}U_{xj0} \end{bmatrix} \\ &\boldsymbol{A}_{j1} = \begin{bmatrix} 0 & -\Delta k_{ij}U_{j0} \\ 0 & -\Delta k_{pj}U_{j0} \end{bmatrix}, \quad \boldsymbol{B}_{j1} = \frac{1}{U_{j0}}\begin{bmatrix} -\Delta k_{ij}U_{yj0} & \Delta k_{ij}U_{xj0} \\ -\Delta k_{pj}U_{yj0} & \Delta k_{pj}U_{xj0} \end{bmatrix} \\ &\boldsymbol{C}_j = \begin{bmatrix} 0 & -I_{y0} \\ 0 & I_{x0} \end{bmatrix}, \quad \boldsymbol{\delta}_j = \begin{bmatrix} \delta_{ij} & 0 \\ 0 & \delta_{pj} \end{bmatrix} \end{aligned} \tag{3}$$

where a superscript dot denotes a time derivative, Δ denotes the small increment of a vector; $\boldsymbol{X}_j$ denotes the state column vector of the j-th converter; $\boldsymbol{A}_j$, $\boldsymbol{B}_j$, and $\boldsymbol{C}_j$ represent the state matrix, control matrix, and output matrix corresponding to the j-th converter; $\boldsymbol{U}_j = [U_{x,j}, U_{y,j}]^T$ and $\boldsymbol{I}_j = [I_{x,j}, I_{y,j}]^T$ are the terminal voltage and output current of the j-th converter expressed in the common x-y coordinate, and $U_j = (U_{x,j}^2 + U_{y,j}^2)^{0.5}$; the subscript 0 denotes the steady-state value of the variables; S_{Bj} represents the operating power of the j-th converter.

The dynamic model of the HMCS grid can be represented by:

$$\Delta\boldsymbol{U} = (\boldsymbol{Z}\otimes\boldsymbol{\alpha}(s))\Delta\boldsymbol{I}, \boldsymbol{\alpha}(s) = \begin{bmatrix} (s+\tau)/\omega_0 & -1 \\ 1 & (s+\tau)/\omega_0 \end{bmatrix} \tag{4}$$

where $\boldsymbol{Z}$ is the node impedance matrix of the power network after eliminating the internal passive nodes; s is the Laplace operator; τ is the ratio of the line resistance to line inductance (i.e., $\tau = R/L$) in the power network.

By combining (2) and (4), the closed-loop model of the HMCS can be obtained:

$$(s\boldsymbol{I} - \boldsymbol{A}_{\text{sys}}(s,\boldsymbol{\delta}))\Delta\boldsymbol{X} = 0 \tag{5}$$

where:

$$\begin{aligned} \boldsymbol{A}_{\text{sys}}(s,\boldsymbol{\delta}) &= \boldsymbol{A}_{\text{sys0}} + \boldsymbol{\delta}\boldsymbol{A}_{\text{sys1}}, \boldsymbol{\delta} = \text{diag}(\boldsymbol{\delta}_j) \\ \boldsymbol{A}_{\text{sys0}}(s) &= \text{diag}(\boldsymbol{A}_{j0}) + \text{diag}(\boldsymbol{B}_{j0})\boldsymbol{K}_\alpha(s) \\ \boldsymbol{A}_{\text{sys1}}(s) &= \text{diag}(\boldsymbol{A}_{j1}) + \text{diag}(\boldsymbol{B}_{j1})\boldsymbol{K}_\alpha(s) \end{aligned} \tag{6}$$

where $\boldsymbol{K}_\alpha(s) = \boldsymbol{Z}[\text{diag}(S_{Bj})\otimes\boldsymbol{\alpha}(s)]\text{diag}(\boldsymbol{C}_j)$, $\boldsymbol{X}$ is the state column vector of the system. $\boldsymbol{A}_{\text{sys}}(s,\boldsymbol{\delta})$ is the characteristic matrix of the HMCS. $\boldsymbol{A}_{\text{sys0}}(s)$ is the nominal characteristic matrix, $\boldsymbol{A}_{\text{sys1}}(s)$ is the uncertainty characteristic matrix, and $\boldsymbol{\delta}$ is the uncertainty matrix of adjustable parameters. The small-signal stability of the HMCS is determined by the roots of the characteristic equation $\det(s\boldsymbol{I} - \boldsymbol{A}_{\text{sys}}(s,\boldsymbol{\delta})) = 0$.

B. Uncertainty Separation and Dimension Reduction

Due to the high dimensionality of $\boldsymbol{A}_{\text{sys}}(s,\boldsymbol{\delta})$ and the coupling of uncertainty with the characteristic matrix, direct robust stability analysis is computationally complex. Assuming the nominal system is stable, the characteristic equation can be equivalently expressed as:

$$\begin{aligned} &\det((s\boldsymbol{I}_{2n} - \boldsymbol{A}_{\text{sys0}}) - \boldsymbol{\delta}\boldsymbol{A}_{\text{sys1}}) = 0 \Leftrightarrow \\ &\det(\boldsymbol{I}_{2n} - \boldsymbol{\delta}\boldsymbol{M}(s)) = 0, \boldsymbol{M}(s) = \boldsymbol{A}_{\text{sys1}}(s\boldsymbol{I}_{2n} - \boldsymbol{A}_{\text{sys0}})^{-1} \end{aligned} \tag{7}$$

where $\boldsymbol{I}_{2n}$ is the $2n$-dimensional identity matrix, $\boldsymbol{M}(s)$ is the $2n \times 2n$ closed-loop system frequency response matrix, and the uncertainty is completely separated into a diagonal matrix $\boldsymbol{\delta}$.

In practice, only specific critical converters require uncertainty analysis. Considering the parameter adjustment of the first m ($m \leq n$) converters (which can be any m converters through matrix transformation), the characteristic equation is equivalent to:

$$\begin{aligned} &\det\left(\boldsymbol{I}_{2n} - \begin{bmatrix} \boldsymbol{\delta}_u & \boldsymbol{0} \\ \boldsymbol{0} & \boldsymbol{0} \end{bmatrix}\begin{bmatrix} \boldsymbol{M}_{11}(s) & \boldsymbol{M}_{12}(s) \\ \boldsymbol{M}_{21}(s) & \boldsymbol{M}_{22}(s) \end{bmatrix}\right) = 0 \\ &\Leftrightarrow \det\left(\begin{bmatrix} \boldsymbol{I}_{2m} - \boldsymbol{\delta}_u\boldsymbol{M}_{11}(s) & -\boldsymbol{\delta}_u\boldsymbol{M}_{12}(s) \\ \boldsymbol{0} & \boldsymbol{I}_{2(n-m)} \end{bmatrix}\right) \\ &\Leftrightarrow \det(\boldsymbol{I}_{2m} - \boldsymbol{\delta}_u\boldsymbol{M}_{11}(s)) = 0 \end{aligned} \tag{8}$$

where $\boldsymbol{\delta}_u = \operatorname{diag}(\delta_{i1}, \delta_{p1}, \ldots, \delta_{im}, \delta_{pm})$, includes only the uncertainty of the m converters of interest. $\boldsymbol{M}_{11}(s)$ is the upper-left $2m \times 2m$ block submatrix of $\boldsymbol{M}(s)$, and other sub-blocks are defined similarly.

The HMCS uncertainty separation model has the advantages of being low-dimensional and approximation-free, providing a foundation for robust stability analysis combined with value set theory.

III. HMCS Parameter Analysis Method

A. Robust Stability Analysis of HMCS Parameters

This section utilizes the uncertainty separation model and the value set graphical method for robust stability analysis. Within the entire adjustable parameter space $\mathcal{D}$, the value set $T(s)$ is defined as the set of values in the complex plane:

$$T(s) = \{\det(\boldsymbol{I}_{2m} - \boldsymbol{\delta}_u \boldsymbol{M}_{11}(s)) : \boldsymbol{\delta}_u \in \mathcal{D}\} \tag{9}$$

Based on the zero exclusion principle [8], assuming the nominal system $\boldsymbol{M}_{11}(s)$ is stable, the robust stability of the entire system within the adjustable parameter range is guaranteed if and only if the value set $T(j\omega)$ excludes the origin $(0,0)$ for all $\omega \geq 0$. Mathematically, the inclusion of the origin in $T(j\omega)$ signifies the existence of characteristic roots on the imaginary axis. Physically, this critical state implies that the system's equivalent damping has vanished, depriving it of the capability to suppress oscillations.

Since direct calculation over the infinite continuous space $\mathcal{D}$ is computationally prohibitive, the multilinear property of the characteristic polynomial with respect to the uncertainty variables $\boldsymbol{\delta}_u$ is exploited. According to the mapping theorem [9], the value set is entirely contained within the convex hull formed by the images of the vertices of $\mathcal{D}$. Consequently, the convex hull of $T(j\omega)$ is rigorously defined by the images of the 2^m vertices, which represent the extreme parameter combinations:

$$\operatorname{co}(T(j\omega)) = \operatorname{co}(\{\det(\boldsymbol{I}_{2m} - \boldsymbol{\delta}_u(V_r)\boldsymbol{M}_{11}(j\omega)) : V_r \in \operatorname{ve}(\mathcal{D})\}) \tag{10}$$

where co denotes the convex hull and ve denotes the vertices of the parameter space.

It is noteworthy that the mapping theorem only provides a sufficient condition for stability, and its conclusion has a certain degree of conservatism. As shown in Fig. 1, the boundary where the convex hull intersects the origin does not necessarily correspond to the true boundary of the value set. To compensate for this limitation, this paper introduces the multivariable stability margin $k_m(j\omega)$, defined as the maximum variation range under which the system remains stable. As $k_m(j\omega)$ increases, the range of $T(j\omega)$ expands monotonically. The value of $k_m(j\omega)$ that makes $T(j\omega)$ first touch the origin is the stability margin at the corresponding frequency ω:

$$k_m(j\omega) = \inf\{k \in [0, \infty) \mid \det(\boldsymbol{I}_{2m} - k\boldsymbol{\delta}_u \boldsymbol{M}_{11}(j\omega)) = 0, \; \boldsymbol{\delta}_u \in \mathcal{D}\} \tag{11}$$

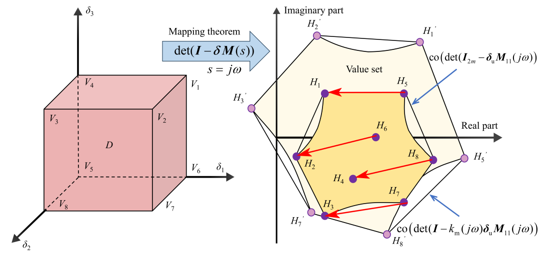

Fig. 1. Mapping theorem and the convex hull of the value set.

The computation of $k_m(j\omega)$ employs an iterative approximation algorithm characterized by converging lower and upper bounds. Specifically, the lower bound of the stability margin is determined when the convex hull of the value set first intercepts the origin, while the upper bound is identified when the origin is intercepted by the vertex paths. Through an iterative domain-splitting process where the parameter domain is continuously subdivided, these bounds asymptotically converge to the exact k_m, thereby eliminating computational conservatism. Specific algorithmic steps can be found in relevant works [10]. The minimum value among the calculated $k_m(j\omega)$ at all frequencies is defined as the system's robust stability margin, K_m.

When $K_m > 1$, the system is robustly stable within the given parameter adjustment range; when $K_m \leq 1$, the system has a potential risk of instability. Furthermore, the frequency ω_c corresponding to the minimum point of $k_m(j\omega)$ is the dominant unstable oscillation frequency of the HMCS, providing an accurate basis for subsequent parameter tuning optimization.

B. Parameter Tuning Strategy

Through K_m, it is possible not only to determine stability but also to find the parameter combination for marginal instability at the minimum parameter variation range of the HMCS. Under the K_m-times parameter variation range, the uncertain parameter combination corresponding to $T(j\omega_c)$ first touching the origin is denoted as $\boldsymbol{\delta}_c$, satisfying:

$$\det(\boldsymbol{I}_{2m} - K_m \boldsymbol{\delta}_c \boldsymbol{M}_{11}(j\omega_c)) = 0, \boldsymbol{\delta}_c \in \mathcal{D} \tag{12}$$

It is clear that $K_m\boldsymbol{\delta}_c$ is the critical instability parameter combination under the minimum parameter adjustment range for HMCS. At this point, if the influence direction of each parameter on HMCS stability can be determined, a parameter tuning decision can be made to avoid system instability and enhance system strength.

A strategy is proposed to determine parameter adjustments by observing the movement direction of $T(s)$ near ω_c. To evaluate a specific parameter, other uncertain parameters are fixed at a vertex combination of $\mathcal{D}$. As shown in Fig. 1, the arrow's direction indicates the movement trend of the value set in the complex plane as the parameter of interest increases. If the value set moves towards the origin, the system's stability deteriorates. Conversely, if the value set

TABLE I
PARAMETERS OF CONVERTERS

Parameter	Value
Filter inductance, filter capacitance, dc capacitance	0.05, 0.05, 0.038 p.u.
PI parameters of current control loop	1, 10
PI parameters of the active power control loop	0.5, 5
Parameters of the voltage feedforward filter	0.0005
The steady-state value of P_0, Q_0 of each converter	1.0 p.u., 0 p.u.

TABLE II
PLL PI PARAMETERS AND RATED POWER OF CONVERTERS

Converter j	1	2	3	4	5	6	7	8	9
$k_{i,j}$	9000	9000	8600	8600	10000	10000	10000	10000	10000
$k_{p,j}$	18	18	20	20	25	25	20	20	20
P_j (MW)	1	1.7	1	1	1	1	1	1	1.5

moves away from the origin, the system's stability is enhanced, and the corresponding parameter adjustment direction is the direction of system strength enhancement.

It is worth mentioning that when $K_m < 1$, the value set envelope already contains the origin. To accurately and intuitively judge the impact of parameter adjustments on the value set's direction, a negative damping line with damping ratio ζ can be introduced in the complex plane:

$$s_g = -\frac{\zeta\omega}{\sqrt{1-\zeta^2}} + j\omega \tag{13}$$

By considering a negative damping ratio ζ and calculating $T(s_g)$, $T(s_g)$ will no longer contain the origin. Analyzing the parameter adjustment direction of $T(s_g)$ is equally accurate because the imaginary axis can be seen as a special case of the damping line with $\zeta = 0$. Since the response of eigenvalues to parameter changes is continuous, a parameter adjustment direction that can move an eigenvalue from $\zeta < 0$ back to the stable damping region must also be able to move it across the imaginary axis to the negative real part region.

The value set analysis method proposed in this paper can accurately consider the synergistic changes and interactions of multiple parameters simultaneously. The next section will demonstrate the impact of HMCS parameters on system strength through the application of this method.

IV. CASE STUDY

This section aims to apply the proposed parameter analysis method to investigate the complex impact of HMCS parameters on system strength and to validate the effectiveness of the parameter optimization strategy. An electromagnetic transient simulation model of the New England 39-bus power system is established for this investigation.

In this system, 9 converters equipped with PLLs are interconnected through the 39-bus meshed network. The network parameters are consistent with the standard IEEE 39-bus system cited in [11] . The control parameters of the converters are detailed in Tables I and II.

The PLL parameters of the 2nd and 9th converters are selected as adjustment objects, with a parameter adjustment

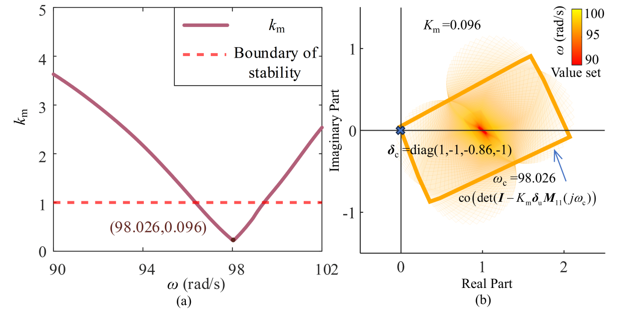

Fig. 2. k_m plot and the value set plot of $\det(\boldsymbol{I} - K_m \boldsymbol{\delta}_u \boldsymbol{M}_{11}(j\omega))$.

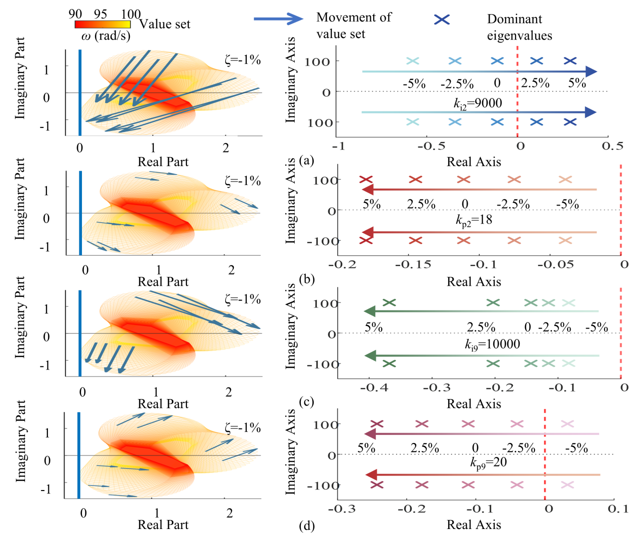

Fig. 3. Value set movement direction and dominant eigenvalues as (a) δ_{i2}, (b) δ_{p2}, (c) δ_{i9}, (d) δ_{p9} increase from -1 to 1.

range of $\pm 5\%$. Based on the uncertainty separation model, the stability is assessed using the K_m theory, as shown in Fig. 2.

Fig. 2(a) shows that k_m is minimal at $\omega_c = 98.026$ rad/s. The system's $K_m < 1$, indicating that the HMCS is robustly unstable within the $\pm 5\%$ parameter variation range. Furthermore, Fig. 2(b) shows the value set at K_m. The parameter combination where the value set first touches the origin is $\boldsymbol{\delta}_c$. Converting $K_m \boldsymbol{\delta}_c$ to actual parameters yields a set of critical instability parameters under the minimum parameter adjustment range for HMCS: $k_{i2} = 9043.3$, $k_{p2} = 17.9$, $k_{i9} = 9958.5$, $k_{p9} = 19.9$.

Next, a parameter tuning strategy is presented. Since the HMCS is robustly unstable, a $\zeta = -1\%$ is introduced to analyze the trend of the value set near ω_c. Fig. 3 shows the value set movement direction and the corresponding dominant eigenvalues of the system as each uncertain parameter δ_{i2}, δ_{i9}, δ_{p2}, and δ_{p9} increases from -1 to 1.

Fig. 3(a) shows that as δ_{i2} increases, $T(s)$ moves closer to the origin, and the system strength weakens. The real part of the corresponding dominant eigenvalue increases, which is consistent with the $T(s)$ analysis. Figs. 3(b), (c), and (d) show

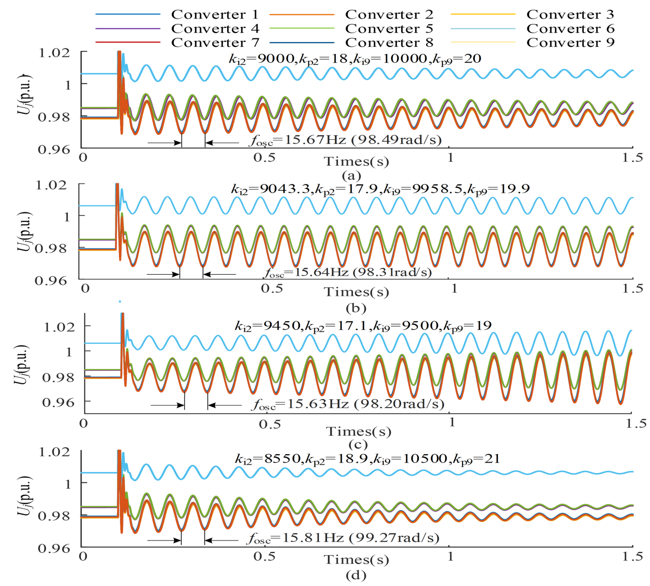

Fig. 4. Time-domain waveforms of converter terminal voltage.

that as k_{p2}, k_{i9}, and k_{p9} increase, $T(s)$ moves away from the origin, the real part of the dominant eigenvalues decreases, and the system strength is enhanced. The dominant eigenvalue plots confirm that the parameter analysis remains accurate after introducing a negative ζ. At this point, combined with the critical instability parameter combination, an appropriate parameter tuning strategy can be given to avoid the instability combination.

To further verify the accuracy of the robust stability analysis and the effectiveness of the parameter adjustments, time-domain simulations were performed on the system. At $t = 0.1$ s, a 0.05 p.u. voltage swell was applied to the AC grid bus and quickly cleared. The converter voltage waveforms under different parameter adjustments are shown in Fig. 4.

Fig. 4(a) shows the system response under nominal parameters; the system tends to be stable but with very weak system strength. Fig. 4(b) uses the critical instability parameter combination determined by $K_m\boldsymbol{\delta}_c$; the voltage waveform shows approximately critical oscillation, verifying the accuracy of K_m in judging HMCS robust stability. Fig. 4(c) shows the parameters adjusted by 5% in the direction of $T(s)$ moving towards the origin; the voltage waveform shows divergent oscillation, indicating that further worsening the parameters from the critical instability combination will lead to system instability. Fig. 4(d) shows the parameters adjusted by 5% in the direction of $T(s)$ moving away from the origin; the system strength is significantly increased. The simulation results strongly validate that the method proposed in this paper can accurately determine the system's robust stability and provide an effective parameter tuning strategy to enhance system strength.

Furthermore, this case study reveals that the adjustment of the same type of parameters in different converters, such as k_{i2} and k_{i9}, has opposite effects on system strength. This illustrates the complex influence of converter parameter adjustments in HMCS, and a unified tuning strategy cannot be given.

V. Conclusion

This paper proposed a robust stability analysis method and parameter tuning strategy for PLL-dominated HMCS systems based on converter parameters. The analysis confirms that converter coupling leads to non-uniform tuning rules , where identical parameters in different converters can have opposite effects on system strength. Furthermore, the research results show that even minor adjustments to key converter parameters can either destabilize the system or enhance its system strength. The method proposed in this paper provides a theoretical basis and practical guidance for small-signal stability assessment and converter parameter optimization in practical engineering. Future research will focus on the optimal solution for HMCS parameter tuning combinations.

References

[1] Q. Shi, W. Dong, G. Wang, J. Ma, C. Wang, X. Guo, and V. Terzija, "Grid strength assessment method for evaluating small-signal synchronization stability of grid-following and grid-forming converters integrated systems," *Journal of Modern Power Systems and Clean Energy*, 2025.

[2] N. Goñi, J. Marcos, M. García, A. García, L. Marroyo, and A. Urtasun, "Accurate state space grid-following inverter model for small signal stability analysis in converter based power systems," in *2024 International Conference on Renewable Energies and Smart Technologies (REST)*. IEEE, 2024, pp. 1–5.

[3] P. Zhou, J. Yan, R. Song, Y. Li, T. Liu, and W. Xiang, "Frequency-coupled impedance modeling and stability analysis of multiple grid-connected voltage-source converters," in *2021 International Conference on Power System Technology (POWERCON)*. IEEE, 2021, pp. 1202–1207.

[4] Y. Zhou, H. Xin, D. Wu, F. Liu, Z. Li, G. Wang, H. Yuan, and P. Ju, "Small-signal stability assessment of heterogeneous grid-following converter power systems based on grid strength analysis," *IEEE Transactions on Power Systems*, vol. 38, no. 3, pp. 2566–2579, 2022.

[5] J. Xu, Z. Ling, Y. Luo, J. Kan, H. Diao, and S. Xie, "Synchronization stability analysis and parameter design of grid-following inverters considering the interactions of current control and phase-locked loop," *IEEE Journal of Emerging and Selected Topics in Power Electronics*, 2024.

[6] J. Zhou, P. Shi, D. Gan, Y. Xu, H. Xin, C. Jiang, H. Xie, and T. Wu, "Large-scale power system robust stability analysis based on value set approach," *IEEE Transactions on Power Systems*, vol. 32, no. 5, pp. 4012–4023, 2017.

[7] Y. Zhou, H. Xin, D. Wu, G. Wang, H. Yuan, and P. Ju, "Small-signal stability boundary of heterogeneous multi-converter power systems dominated by the phase-locked loops' dynamics," *IEEE Transactions on Energy Conversion*, vol. 37, no. 4, pp. 2874–2888, 2022.

[8] P. Shi, C. Jiang, D. Gan, H. Xin, L. Jia, X. Gao, Y. Xu, and H. Xie, "New value set approach for robust stability of power systems with wind power penetration," *IEEE Transactions on Sustainable Energy*, vol. 10, no. 2, pp. 811–821, 2018.

[9] B. R. Barmish, *New tools for robustness of linear systems*. New York: Macmillan, 1994.

[10] R. R. De Gaston and M. G. Safonov, "Exact calculation of the multiloop stability margin," *IEEE Transactions on Automatic Control*, vol. 33, no. 2, pp. 156–171, 1988.

[11] Y. Tang, G. Hu, Y. Zhang, T. Liu, Z. Fu, and H. Xin, "Online quantification method for system strength of heterogeneous multi-converters power systems from a small signal stability perspective," in *2025 IEEE Power & Energy Society General Meeting (PESGM)*, 2025, pp. 1–5.